Fiber chirped pulse amplification of a short wavelength mode-locked thulium-doped fiber laser

Can Li, Xiaoming Wei,[a] Cihang Kong, Sisi Tan, Nan Chen, Jiqiang Kang, and Kenneth K. Y. Wong[b]
Department of Electrical and Electronic Engineering, The University of Hong Kong, Pokfulam Road, Hong Kong

(Received 17 July 2017; accepted 13 November 2017; published online 8 December 2017)

Exploiting the promising third near-infrared optical window (1600–1870 nm) for deep bioimaging is largely underdeveloped, mostly because of the lack of stable femtosecond laser sources in leveraging the less scattering loss and locally reduced water absorption. In this letter, we demonstrate the fiber chirped pulse amplification of a short wavelength mode-locked thulium-doped fiber laser (TDFL) at 1785 nm. The mode-locked TDFL (via nonlinear polarization rotation) operates stably at the soliton pulsing regime with a fundamental repetition rate of 46.375 MHz. Utilizing a two-stage fiber amplifier incorporated along the pulse chirping fiber, the power of the laser pulse is boosted up to 690 mW. After dechirping with a diffraction grating pair, laser pulse with a duration of 445 fs, pulse energy of 5.7 nJ, and peak power of 12 kW is achieved. Higher power can be achieved by exploiting low-loss high power fiber components at this special wavelength range. https://doi.org/10.1063/1.4996441

In recent years, the bioimaging community has been accessing the third near-infrared (NIR3) optical window (1600–1870 nm) thanks to the advancements of corresponding fiber laser technologies. Compared with shorter wavelengths, the NIR3 optical window has the merits of reduced optical attenuation and diminished phototoxicity and is therefore advantageous for imaging of deep and turbid scattering tissues.[1,2] Up to now, a series of imaging modalities such as optical coherence tomography,[3] three-photon microscopy,[4] and optical coherence microscopy[5] have been demonstrated at the 1700 nm optical band. However, the laser sources adopted in these systems were obtained via nonlinear wavelength conversion of ultrafast lasers at the well-developed telecommunication band like supercontinuum generation (SCG)[3,5] and Raman soliton self-frequency shift (SSFS),[4] which would degrade the original source performances and raise the issue of stability and noise.[6,7] To obtain more desirable laser sources at this wavelength region, an alternative is to directly construct laser cavity by exploiting the optical gain of thulium-doped fiber (TDF), of which the energy level transition $^3F_4 \rightarrow {}^3H_6$ covers a wideband from 1600 nm to over 2100 nm.[8,9] Thulium-doped fiber laser (TDFL) is a versatile platform that can produce various sources in the eye-safe region with engineered performances. Nevertheless, the quasi-three-level nature of TDF emission leads to strong reabsorption of the light at short wavelengths that generally shift the operating wavelength of TDFL to longer ones, typically >1900 nm.[10,11]

Few research efforts have devoted to obtaining TDFLs lasing at the short wavelengths (<1800 nm), with the motivation of promising applications relating to the rich molecular absorption lines in this region.[12,13] In addition, the short wavelength thulium-doped fiber amplifier (TDFA) has also attracted research interests owing to its potential in extending the wavelength window for optical communications.[14,15] The general methods include high fractional exciting of the gain fiber with

[a]Present address: Department of Medical Engineering, California Institute of Technology, 1200 East California Boulevard, Pasadena, California 91125, USA.
[b]Author to whom correspondence should be addressed: kywong@eee.hku.hk

an in-band pump source, employing narrowband wavelength selective filter, and suppressing the unwanted amplified spontaneous emission (ASE) at the long wavelength. Nevertheless, current works mainly involve laser sources operating in the continuous-wave (CW) regime with narrow bandwidth. Regarding the applications in bioimaging, a pulsed source with considerable short duration and high peak power is highly desirable. Previously, we have demonstrated a high power and widely tunable nanosecond short-wave infrared (SWIR) laser by implementing a thulium-assisted optical parametric oscillator (TAOPO).[16] The energetic and broadband emission capability of TDF at wavelengths <1800 nm revealed in this system implies that it is competent in yielding high power ultrafast laser sources at the short wavelength side. At present, the only report about the sub-1800 nm ultrafast laser that exploiting the fundamental transition of thulium ions is a thulium-holmium mode-locked fiber laser enabled by an acousto-optical tunable filter (AOTF) with a limited 3 dB bandwidth of 3 nm.[17]

In this letter, we demonstrated a short wavelength fundamentally mode-locked TDFL at 1785 nm and subsequently magnified its power with a fiber chirped pulse amplification (CPA) scheme. Laser pulse with an average power of 690 mW and repetition rate of 46.375 MHz was realized. Then the duration of the amplified pulse was compressed to 445 fs with a pulse energy of 5.7 nJ and peak power of 12 kW by implementing a pulse compressor with a diffraction grating pair (GP).

Figure 1(a) depicts the schematic of the short wavelength mode-locked TDFL associated with the CPA system. The ring cavity of the TDFL was built by a fusion type 2 × 2 wavelength-division multiplexer coupler (WDMC). The gain fiber was a segment of 0.8-m-long TDF (OFS TmDF200), which was pumped by P1—an erbium-doped fiber amplifier (EDFA) with seed source from a 1560 nm tunable laser source (TLS)—through one port of the WDMC. Mode-locking of the laser was initiated and maintained by the association of two quarter-wave plates (QWP), a half-wave plate (HWP), and a polarization sensitive isolator (ISO) through the effect of nonlinear polarization rotation (NPR). Two fiber collimators (COLs) together with a silver coated mirror (M) and a long-pass dichroic mirror (DM) were utilized to direct light between the fiber part and the NPR assembly and complete the cavity. The total length of optical fiber in the cavity was about 4.3 m, while that of the free-space part was 0.3 m. The DM has a cutoff wavelength of 1800 nm and was configured to dump the light at wavelengths >1800 nm and force the laser to operate at the short wavelength regime. The laser signal centered 1785 nm was extracted from the cavity via the last port of the WDMC with a coupling ratio of about 3 dB (50%), which was measured with a homemade supercontinuum source, as shown in Fig. 1(b). The pump loss spectrum of the WDMC is also shown in the figure, indicating a pumping

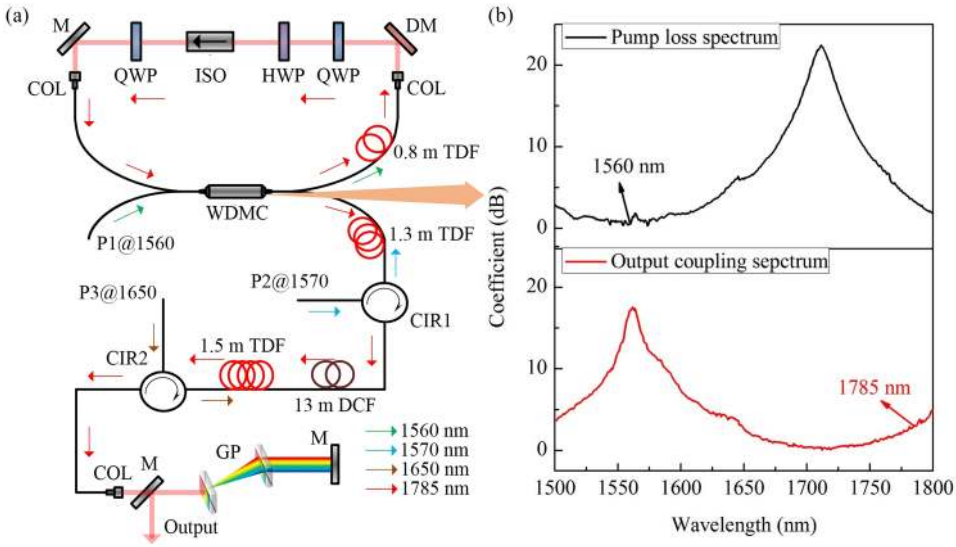

FIG. 1. (a) The schematic of the short wavelength mode-locked TDFL associated with the CPA system. (b) The measured pump loss spectra and output coupling of the WDMC with a homemade supercontinuum source.

loss coefficient of 0.7 dB (15%) at 1560 nm, while the rest of the pump power was coupled into the laser cavity. In view of this, there will be some power component from the 1560 nm pump presenting at the output port of the cavity, and it would affect the subsequent characterization of the laser source. To address this problem, a 10-m-long erbium-doped fiber (EDF, Liekki, ER80-8/125) was employed to absorb the residual pump before conducting measurement on the optical spectrum, RF spectrum, and pulse train, of which the effect of EDF should be neglected.

Under appropriate settings of the wave plates, stable self-starting 3rd order harmonic mode-locking of the laser was obtained when the launched pump power reached 380 mW, after the processes of CW and unstable pulsing operation. Then the laser switched to the fundamental mode-locking regime when the pump power was gradually decreased to around 240 mW, corresponding to an output power of 3.5 mW. The laser spectrum was measured with an optical spectrum analyzer (OSA, Yokogawa, AQ6375) under a resolution of 0.5 nm, as shown in Fig. 2(a). The spectral peaks symmetrically located on both sides of the central wavelength indicate a soliton pulsing mechanism in the cavity. The full width at half maximum (FWHM) of the spectrum was 6.8 nm, corresponding to a transform-limited pulse duration of 492 fs, assuming a sech^2 pulse profile. The RF spectrum of the fundamental repetition rate of 46.375 MHz is shown in Fig. 2(b), with a resolution bandwidth of 100 Hz and a scanning span of 100 kHz. The signal-to-noise ratio (SNR) was larger than 74 dB, indicating the stable operation of the mode-locked laser. Figure 2(c) depicts the oscilloscope trace of the pulse train with a period of 21.6 ns, confirming the fundamental mode-locking operation.

To amplify the laser signal, the output port of the WDMC was first fusion spliced to a 1.3-m-long TDF, which was then connected to the port 2 of a circulator (CIR1). A 1570 nm TLS seeded EDFA (P2) was utilized to backward pump the TDF through the port 1 of CIR1. With 400 mW pump power been launched into the TDF, about 80 mW signal power was recorded at the port 3 of CIR1. At this point, the residual 1560 nm pump power from the laser cavity was completely depleted by the TDF. It is worth noting that the pump power from P2 was verified to be basically absorbed by the TDF by adding an extra circulator between the WDMC and the TDF. It was removed in Fig. 1(a) because the circulators employed in this work were originally designed for the telecommunication band and would introduce an insertion loss of about 2 dB to the laser signal.[16] The optical spectrum of the amplified laser after CIR1 is shown in Fig. 3(a). It was observed that the FWHM was slightly broadened to about 11 nm, owing to the effect of self-phase modulation (SPM). In addition, significant ASE at wavelengths longer than 1800 nm was raised, caused by the reabsorption effect of TDF.

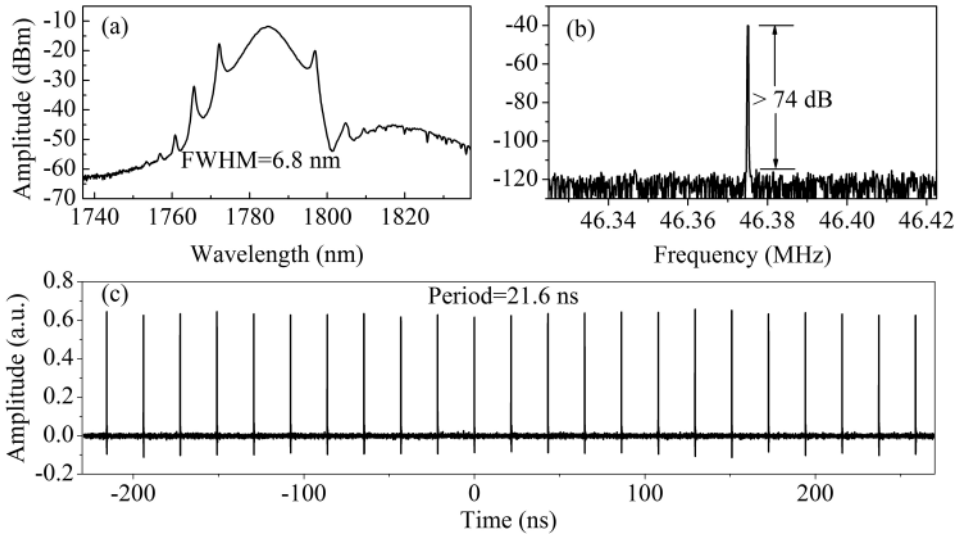

FIG. 2. Characterization of the mode-locked TDFL: (a) optical spectrum; (b) RF spectrum; (c) oscilloscope trace of the pulse train.

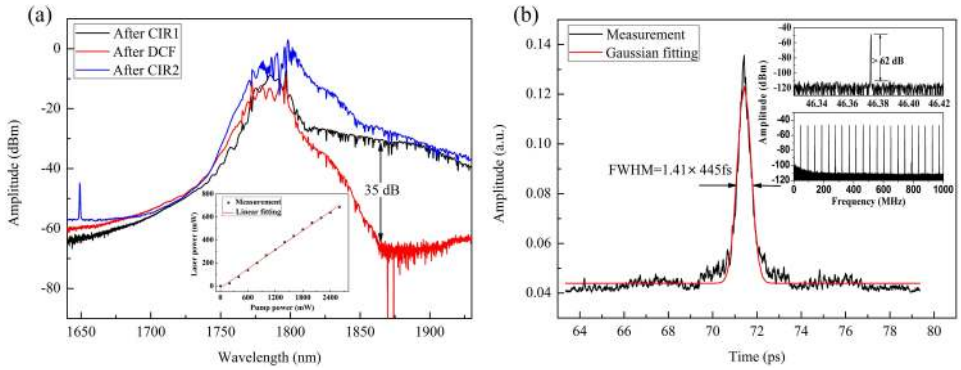

FIG. 3. (a) The optical spectra of the laser signal after CIR1, DCF, and CIR2 with the launched pump power from P2 and P3 are set to be 0.4 W and 2.6 W, respectively. Inset: the measured power of the amplified laser after CIR2 versus the launched pump power from P3 and the corresponding linear fitting curve. (b) AC trace of the compressed pulse: measurement and Gaussian fitting. Inset: RF spectrum of the amplified pulse with maximum power at the fundamental cavity frequency and over 1 GHz frequency range.

Then the port 3 of CIR1 was fusion spliced to a 13-m-long circled (12-cm-long diameter) dispersion-compensating fiber (DCF, OFS, DCM-DK-425) with a group-velocity dispersion of 118 ps^2/km at 1550 nm to chirp the pulse. The length of the DCF was determined to provide sufficient chirping to the pulse while limiting the introduced insertion loss to maintain adequate signal power for the next stage amplification. The optical spectrum after the DCF is demonstrated in Fig. 3(a), in which one can find that the ASE at the long wavelength side was remarkably suppressed with a maximum suppression of 35 dB thanks to the strong wavelength dependent bend loss of the DCF,[14] making the resulted laser signal advantageous for subsequent amplification. The modulation fringes at the vicinity of the center wavelength of the red curve indicate that the laser signal has experienced some degree of SPM effect. Moreover, monitoring of the laser power revealed that the DCF has considerably reduced the average power to ~5 mW, corresponding to an insertion loss of 12 dB, which was attributed to the intrinsic transmission loss of the DCF and splicing loss on both ends of the DCF. Subsequently, the DCF was fusion spliced to another 1.5-m-long TDF to further amplify the laser. A high-power Raman laser (P3) with a wavelength of 1650 nm associated with another circulator (CIR2) was utilized to backward pump the TDF. The inset of Fig. 3(a) demonstrates the power of the laser after CIR2 versus the launched pump power and the corresponding linear fitting curve. The laser power was linearly increased with the enhancement of the pump power. The linear fitting of the measurements indicated that the slope efficiency was 27.7%, which was mainly attributed to the insertion loss of CIR2 for both the pump and laser signal, as an extra circulator was also employed to verify that the launched pump power was almost absorbed by the TDF. At the maximum pump power of 2.6 W (limited by the damaging threshold of CIR2), the realized average power was nearly 690 mW. Considering the insertion loss of CIR2, the actual achieved power should be 1090 mW with a pulse energy of 23.5 nJ. In addition, it is apparent in the figure that the TDF was not saturated yet, implying higher power is achievable given that appropriate components are available. The optical spectrum of the laser at maximum power was measured and shown in Fig. 3(a). From the figure, the FWHM of the spectrum was further widened to about 20 nm. Owing to the high fraction in-band core-pumping of the TDF at its absorption peak (around 1650 nm), the pulse was efficiently amplified with calculated ASE power (integrated from 1850 nm to 1930 nm) to total output power (integrated from 1700 nm to 1930 nm) ratio to be only 0.5%. In addition, the small peak at 1650 nm was resulted from the reflection of the pump from P3 by CIR2.

To compress the duration of the amplified pulse, a transmission diffraction grating pair (GP, LightSmyth, T-940L-2710-92) was utilized to construct a folded Treacy grating compressor to dechirp the pulse. As the operating wavelength of the gratings was 1570-1610 nm (C + L band), its transmission efficiency was deceased from 92% to 79% (~1 dB) in the current experiment. The laser signal was launched into the compressor through a fiber COL, while another COL with a 0.2-m-long fiber patch cord was used to direct the compressed pulse to an autocorrelator (Femtochrome, FR-103MN) to

assess the pulse width. Figure 3(b) demonstrates the measured and the corresponding Gaussian fitted autocorrelation (AC) trace, indicating a compressed pulse width of 445 fs. The slight pedestal should be attributed to the spectral distortion in the amplifier and the positive third order dispersion of the fiber components. In addition, it is observed that the measured autocorrelation trace is a little noisy, and there is 0.04 offset in the ordinate. The reason is that the gain of the built-in photomultiplier tube of the autocorrelator was set to its maximum to obtain the measured AC trace, as it has a very weak response to the corresponding second harmonic signal (~890 nm). After compression, the laser power at the output of the compressor was measured to be 264 mW, corresponding to a pulse energy of 5.7 nJ and a peak power of 12 kW. The inset of Fig. 3(b) shows the RF spectrum of the amplified pulse with maximum power at the fundamental cavity frequency and over 1 GHz frequency range. The observed SNR of >62 dB together with the cleanness and the flatness (<1.5 dB) of the overall spectrum indicate the stable operation of the system.

In conclusion, we have demonstrated the fiber CPA of a short wavelength mode-locked TDFL at 1785 nm. Through engineering the oscillator and the amplifier design, a robust operated laser system was achieved with an output duration of 445 fs, pulse energy of 5.7 nJ, and peak power of 12 kW. Moreover, higher power is achievable through utilizing components that are designed for this special wavelength band. It is believed that this laser source can be a promising candidate for applications in deep bioimaging at the NIR3 optical window over other fiber nonlinear converted sources.

The work described in this paper was partially supported by grants from the Research Grants Council of the HKSAR, China (Project Nos. HKU 17205215 and HKU 17208414), GD-HK Technology Cooperation Funding Scheme GHP/050/14GD, University Development Fund of HKU, Science and Technology Project of Guangdong (Project No. 2014B050505007), and Guangdong Natural Science Foundation Grant, China (Project No. 2014B05050501).

[1] L. A. Sordillo, Y. Pu, S. Pratavieira, Y. Budansky, and R. R. Alfano, J. Biomed. Opt. **19**(5), 056004 (2014).
[2] L. Shi, L. A. Sordillo, A. Rodríguez-Contreras, and R. Alfano, J. Biophoton. **9**(1-2), 38 (2016).
[3] U. Sharma, E. W. Chang, and S. H. Yun, Opt. Express **16**(24), 19712 (2008).
[4] N. G. Horton, K. Wang, D. Kobat, C. G. Clark, F. W. Wise, C. B. Schaffer, and C. Xu, Nat. Photonics **7**, 205 (2013).
[5] M. Yamanaka, T. Teranishi, H. Kawagoe, and N. Nishizawa, Sci. Rep. **6**, 31715 (2016).
[6] X. Wei, C. Zhang, S. Xu, Z. Yang, K. K. Tsia, and K. K. Y. Wong, IEEE J. Sel. Top. Quantum Electron. **20**(5), 7600207 (2014).
[7] S. Pickartz, U. Bandelow, and S. Amiranashvili, Opt. Lett. **42**(7), 1416 (2017).
[8] S. D. Agger and J. H. Povlsen, Opt. Express **14**(1), 50 (2006).
[9] S. D. Jackson, Laser Photonics Rev. **3**(5), 466 (2009).
[10] P. F. Moulton, G. A. Rines, E. V. Slobodtchikov, K. F. Wall, G. Frith, B. Samson, and A. L. G. Carter, IEEE J. Sel. Top. Quantum Electron. **15**(1), 85 (2009).
[11] C. W. Rudy, M. J. F. Digonnet, and R. L. Byer, "Advances in 2-lm Tm-doped mode-locked fiber lasers," Opt. Fiber Technol. **20**(6), 642 (2014).
[12] J. Daniel, N. Simakov, M. Tokurakawa, M. Ibsen, and W. Clarkson, Opt. Express **23**(14), 18269 (2015).
[13] X. Xiao, H. Guo, Z. Yan, H. Wang, Y. Xu, M. Lu, Y. Wang, and B. Peng, Appl. Phys. B **123**(4), 135 (2017).
[14] Z. Li, Y. Jung, J. Daniel, N. Simakov, M. Tokurakawa, P. Shardlow, D. Jain, J. Sahu, A. Heidt, and W. Clarkson, Opt. Lett. **41**(10), 2197 (2016).
[15] J. Wang, S. Liang, Q. Kang, Y. Jung, S.-U. Alam, and D. J. Richardson, Opt. Express **24**(20), 23001 (2016).
[16] C. Li, N. Chen, X. Wei, J. Kang, B. Li, S. Tan, L. Song, and K. K. Wong, Opt. Lett. **41**(22), 5258 (2016).
[17] T. Noronen, O. Okhotnikov, and R. Gumenyuk, Opt. Express **24**(13), 14703 (2016).